DOI https: //doi. org/10.1007/s11595-022-2506-2

High Temperature Tensile Property and Fracture Behavior of Directionally Solidified Fe-Al-Ta Eutectic Composites

CUI Chunjuan[1,3], DENG Li[1], LIU Wei[1], WANG Yan[1], LIU Yue[1], LAI Yuanyuan[1], SU Haijun[2], LIU Yingying[1]

(1.School of Metallurgical Engineering, Xi'an University of Architecture and Technology, Xi'an 710055, China; 2.State Key Laboratory of Solidification Processing, Northwestern Polytechnical University, Xi'an 710072, China; 3. Shaanxi Metallurgical Engineering Technology Research Center, Xi'an 710055, China))

Abstract: Fe-Al-Ta eutectic composites with solidification rates of 6, 20, 30, 80 and 200μm/s were obtained by a modified Bridgman directional solidification technique and alloying. Moreover, tensile property and fracture behavior of Fe-Al-Ta eutectic composites were studied at 600 ℃. The relationship between mechanical property and microstructure at high temperature was studied. Microstructure of Fe-Al-Ta eutectic is composed of Fe_2Ta (Al) Laves phase and Fe (Al, Ta) matrix phase. In addition, the tensile strength at high temperatures is higher than that at room temperature. The tensile strength is increased with the increase of solidification rate. Moreover, fracture morphology transforms from cleavage fracture to dimple fracture as the solidification rate is increased at high temperatures.

Key words: Fe-Al-Ta eutectic; directional solidification; high temperature tensile property; fracture behavior

1 Introduction

Fe-Al intermetallic compound not only has the unique properties of general intermetallic compound, but also its excellent antioxidant and corrosion resistance are comparable to that of stainless steel. Fe-Al intermetallic compound gets more attention due to low density (6.5-7.2 g/cm^3), low price and high strength, and it has a broad application prospect in the fields of aviation, aerospace, energy and chemical industry[1-3]. However, the brittleness at room temperature and the decrease of the strength above 600 ℃ restrict its industrial application[4-8]. Many methods[9-12] have been tried to improve the ductility. Pike *et al*[13] found that Ta-containing Fe_3Al had high creep resistance at temperature of 700 ℃, and the creep times up to about 1 000 h. It is found that the mechanical properties of Fe-40Al are effectively improved after proper heat treatment. Tensile strength of the material quenched at 700 ℃ is 497 MPa[14]. The yield strength and plasticity of the composites are higher than that of the matrix alloy, when Al_2O_3 particles are added into Fe-Al by melting casting[15].

Directional solidification technology[16] can obtain the preferred orientation of the structure and even single crystal, which can significantly improve the properties of the material. High-temperature strength, creep resistance, durability and thermal fatigue properties of the high-temperature engine blade prepared by directional solidification technology have been widely used in aerospace field. Previous works[17-19] have been carried out about microstructure and mechanical properties of Fe-Al-Ta eutectic at room temperature.

Tensile properties and fracture behavior at 600 ℃ high temperature were studied. The influence of solidification rate on mechanical property at high temperature were discussed, and the fracture mechanism were studied as well.

2 Experimental

99.99% of pure iron, 99.999% of pure aluminum and 99.95% pure tantalum were mixed in the vacuum induction melting furnace to get Fe85/Ta7/Al8 (at%)

© Wuhan University of Technology and Springer-Verlag GmbH Germany, Part of Springer Nature 2022

(Received: Mar. 26, 2021; Accepted: Sept. 18, 2021)

CUI Chunjuan(崔春娟): Prof.; Ph D; E-mail: cuichunjuan@xauat.edu.cn

Funded by National Natural Science Foundation of China (No.51201121), Key Industry Innovation Chain (group) Project of Shaanxi Province (No.2019ZDLGY 04-04), International Cooperation Project of Key R&D Program in Shaanxi Province (No.2020KW-033), Industrialization Project of Shaanxi Provincial Department of Education (No.20JC024)

eutectic alloy ingot. The master alloys were obtained by cutting the middle of the ingot into Φ6 mm×100 mm and Φ12 mm×100 mm cylindrical bars. Fe-Al-Ta eutectic composites with different solidification rates were prepared by a modified Bridgman directional solidification technique.

High temperature tensile tests were performed on Fe-Al-Ta eutectic samples with different solidification rates. The testing samples were prepared according to GB/ T4338-2006. The tensile test was carried out on the electronic universal material testing machine with the tensile rate of 0.5 mm/min at 600 ℃.

The high-temperature fracture toughness of Fe-Al-Ta eutectic at different solidification rates were tested by the single-side notched beam (SENB) three-point bending method. The size of the sample was 35 mm×7.5 mm×3.75 mm. The precast crack with 3.75 mm deep and 0.18 mm wide was cut in the middle line of the sample. The precast notch direction was perpendicular to the crystal growth direction.

3 Results and discussion

3.1 Microstructure of the Fe-Al-Ta eutectic

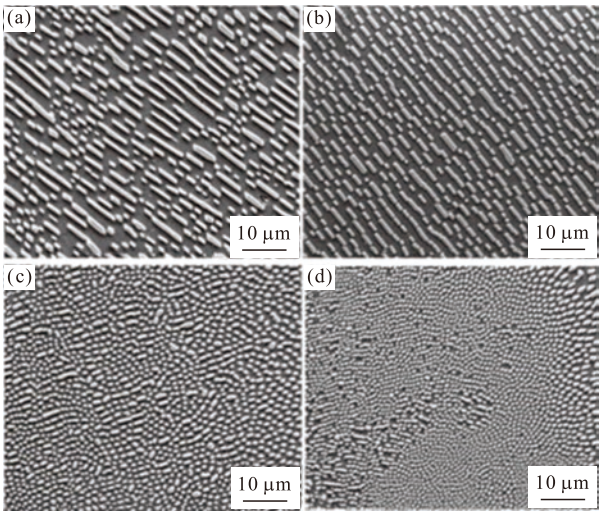

Fig.1 Longitudinal microstructure of Fe-Al-Ta eutectic at different solidification rate: (a)6 μm/s; (b)20 μm/s; (c)30 μm/s; (d)80 μm/s[19]

Fig.1 shows microstructure of Fe-Al-Ta eutectic at different solidification rates[19]. Microstructure is composed of Fe_2Ta (Al) Laves phase in the light phase and Fe (Al, Ta) matrix phase in the dark phase. It can be seen that Laves phases arranged in a fixed direction with obvious anisotropy. Moreover, the solidified structure is gradually refined with the increase of solidification rate. Morphology of Fe-Al-Ta eutectic transforms from broken lamellar eutectic to rod-like eutectic as solidification rate is increased[17].

3.2 High temperature tensile property

Fig.2 shows macrostructures of fracture surfaces of Fe-Al-Ta eutectic at solidification rate of 6, 20, 30 and 80 μm/s, respectively. It can be seen that there is no obvious reduction in the cross-sectional diameter of all specimens. In addition, Fig.2(a) shows that the section is relatively flat. However, tensile section has an obvious inclined angle which is very uneven and irregular as shown in Fig.2(b)-2(d). This indicates that fracture here is influenced by complex stresses.

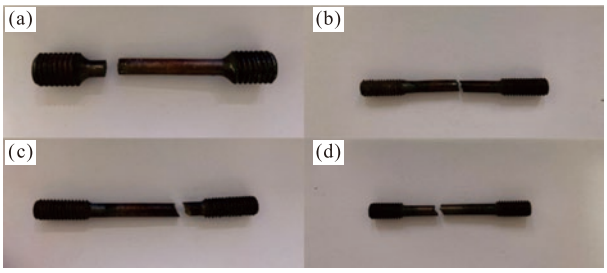

Fig.2 Macrostructures of fracture surfaces of the Fe-Al-Ta eutectic at different solidification rates: (a) 6 μm/s; (b) 20 μm/s; (c) 30 μm/s; (d) 80 μm/s

The stress-strain curves of Fe-Al-Ta eutectic composites with different solidification rates at 600 ℃ are shown in Fig3. Fe-Al-Ta eutectic at solidification rate of 6 μm/s suddenly breaks when the tensile strength of the material reaches the highest value of 341 MPa as Fig.3(a) shows. This indicates a brittle fracture. Fig.3(b) is a stress-strain diagram with the directional solidification rate of 20 μm/s. The tensile strength of Fe-Al-Ta eutectic is 487 MPa. Necking can be observed when the stress gets to the maximum value. The stress-strain curve appears to fall, and then the sample is suddenly broken. There is a phenomenon of pseudo - plasticity in this material. Fig.3(c) shows the stress-strain diagram of Fe-Al-Ta eutectic with solidification rate of 30μm/s, and its tensile strength at 600 ℃ is 507 MPa. The stress-strain curve is similar to that of Fig.3(b) to some extent. The difference between Fig.3 (b) and Fig.3(c) may be caused by the following two reasons. One is the reason of the sample itself. Because there are irregular organization arrangement and a large number of impurities segregation phenomenon in the areas with complex structure such as grain boundary and phase boundary, which may reduce the strength of local areas and makes the sample fracture rapidly; The other is the reason of experimental operation. For example, the tensile test may start without holding for enough time. Fig.3(d) shows the stress-strain diagram

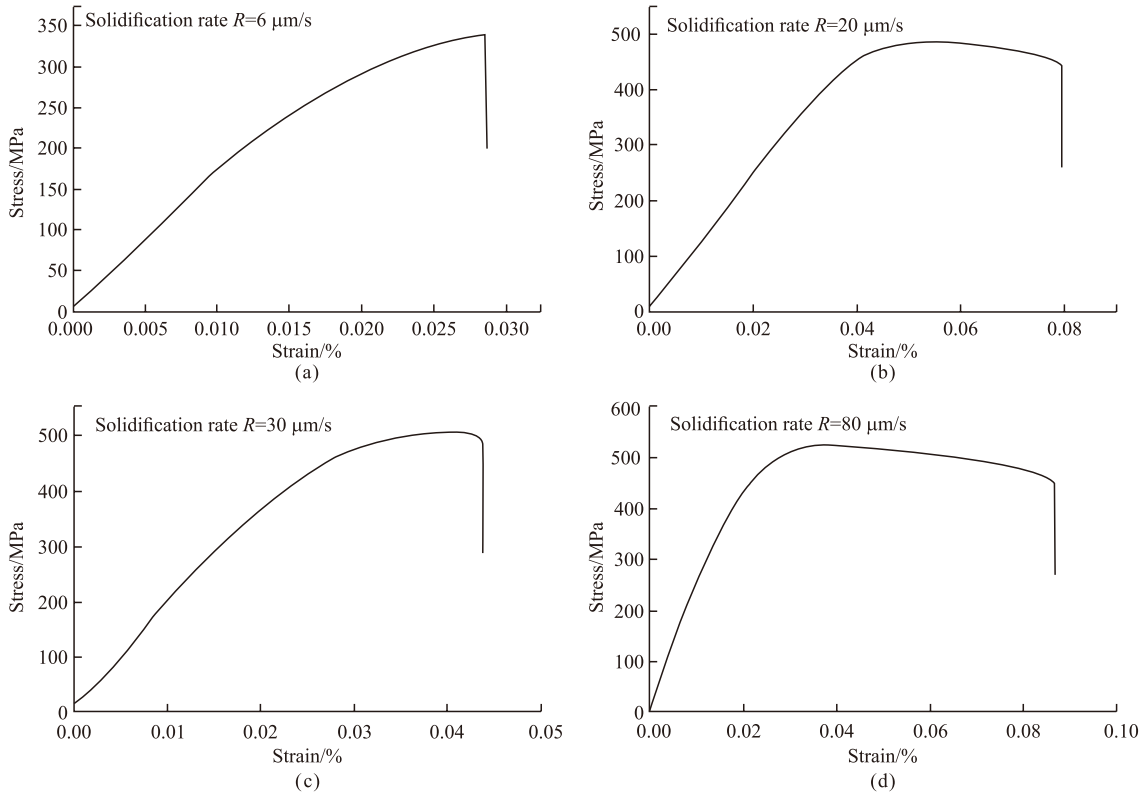

Fig.3 Tensile stress-strain curve of Fe-Al-Ta eutectic at different solidification rates: (a)6 μm/s; (b)20 μm/s; (c)30 μm/s; (d)80 μm/s

Table 1 High temperature tensile properties of the directionally solidified Fe-Al-Ta eutectic

Solidification rate/(μm/s)	Maximum tensile strength/MPa	Elongation after fracture/%	Percentage reduction of area/%
6	341	Brittle fracture	Brittle fracture
20	487	4.5	16
30	507	3.0	9
80	525	5.5	17

of Fe-Al-Ta eutectic composite with solidification rate of 80 μm/s at high temperature of 600 ℃. Fig.3(d) shows a longer curve from maximum load to fracture point as compared with Fig.3(b), indicating that it is a kind of plastic fracture. It can be seen from Fig.1 that the microstructure is refined and sphered with the increase of the solidification rate. Therefore, the plasticity of Fe-Al-Ta eutectic is improved as a result.

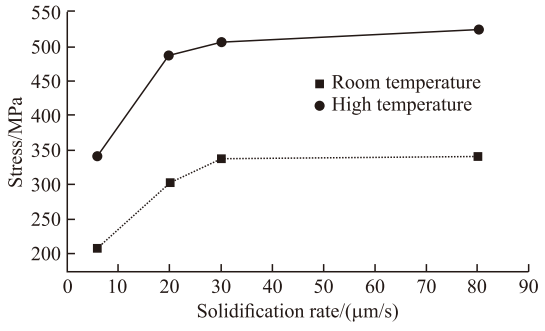

Fig.4 Maximum tensile strength of Fe-Al-Ta eutectic with different solidification rates at room temperature and high temperature

Table 1 shows the tensile properties of Fe-Al-Ta eutectic with different solidification rates at 600 ℃. It can be seen that the tensile strength of directionally solidified Fe-Al-Ta eutectic composite increases with the increase of solidification rate. This is because the microstructure is gradually refined with the increase of solidification rate, and the strength is increased as a result.

Fig.4 is a comparison of tensile strength at room temperature and 600 ℃ high temperature. It can be clearly seen that the tensile strength at high temperature is higher than that at room temperature at the same solidification rate. Generally, the deformation resistance of metal is decreased with the increase of temperature, because the resistance of lattice is decreased and the activity of atom is increased with the increase of temperature. However, the strength of many intermetallic compounds increases firstly and then decreases with the increase of temperature, instead of continuously decreasing due to the formation of Laves phase with L21 structure[20]. The Fe-Al-Ta eutectic investigated in this

paper also belongs to one of them due to the existence of Fe_2Ta (Al) intermetallic phase.

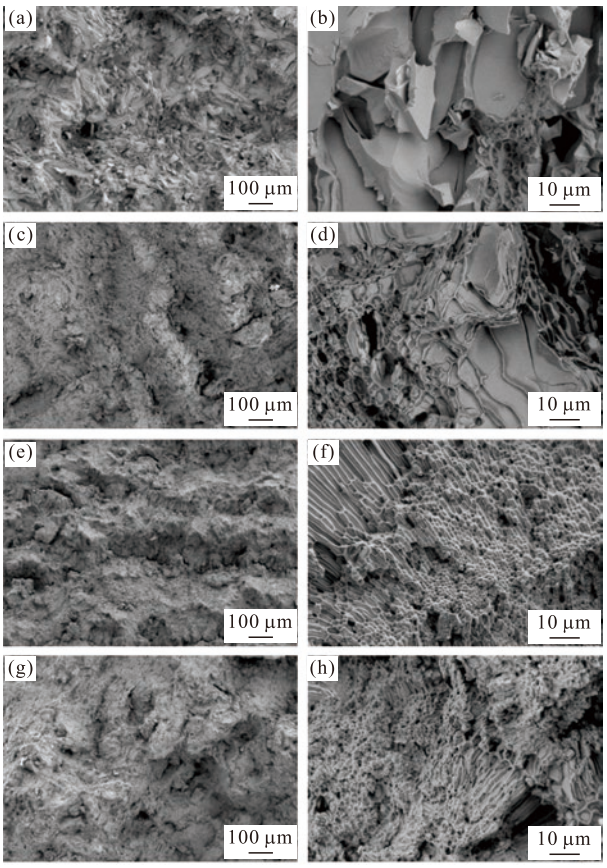

Fig.5 Fracture surfaces of different directionally solidified rate Fe-Al-Ta eutectic after high temperature tensile: (a) -(b) 6 μm/s; (c) -(d) 20 μm/s; (e) -(f)30 μm/s; (g) -(h) 80 μm/s

Fig.5 shows the fracture morphology of Fe-Al-Ta eutectic after high temperature tensile test. Fig.5(a)-(b) are the macroscopic and microscopic fracture morphologies of Fe-Al-Ta eutectic with solidification rate of 6 μm/s after high temperature tensile at a high temperature of 600 ℃. On the macro level, the cross section is uneven, and there is no macroscopic plastic deformation. At the microscopic level, there are a large number of cleavage platforms and a small number of dimples. According to the drawing curve, the fracture mode is brittle fracture. Fig.5(c)-(d) are the macroscopic and microscopic fracture morphologies of Fe-Al-Ta eutectic with solidification rate of 20 μm/s after high temperature tensile at 600 ℃. The cleavage platform and the dimple are observed at the same time, and the elongation after fracture is 4.5%. This indicates that the fracture mode is mixed fracture. Fig.5(e)-(f) are the macroscopic and microscopic fracture morphologies of Fe-Al-Ta eutectic with solidification rate of 30 μm/s after high temperature tensile at 600 ℃. There was no obvious macroscopic plastic deformation before and during fracture. The dimples and the tearing edges around the dimples can be observed in fracture morphology, and the fracture elongation is 3.0%. So, it is considered as a mixed fracture. Fig.5(g)-(h) are the macroscopic and microscopic fracture morphologies of Fe-Al-Ta eutectic with solidification rate of 80 μm/s after high temperature tensile at 600 ℃. It can be seen that the dimples exist and the size is smaller than that of Fe-Al-Ta eutectic with the solidification rate of 30 μm/s. Its fracture elongation rate is 5.5%, and the fracture mode is ductile fracture.

3.3 High temperature fracture toughness

Table 2 shows the data of high temperature fracture toughness. Calculation formula of high temperature fracture toughness K_{IC} is defined as follows:

$$K_{IC}=(F_Q S/BW^{3/2})\times f(a/W) \tag{1}$$

$$S=4W \tag{2}$$

$$f(a/W)=3(a/W)^{1/2}\times \frac{1.99-(a/W)(1-a/W)[2.15-3.93(a/W)+2.70(a/W)^2]}{2(1+2a/W)(1-a/W)^{3/2}} \tag{3}$$

K_{IC} is plane strain fracture toughness, MPa·m$^{1/2}$; W is the height of the sample, mm; B is the thickness of the sample, mm; a is the crack length, mm; S is span, mm, F_Q is the maximum loading force at fracture, kN; $f(a/W)$ is the geometric shape factor of the sample.

The fracture toughness test of metal material is based on the plane strain state at the crack front of the material. If P_{max}/P_q is greater than 1.10, it is believed that the plastic zone at the crack tip is too large and exceeds the condition of small yield range. The theoretical basis and fracture criterion of linear elastic fracture mechanics are no longer applicable, so the measured K_{IC} is invalid [21].

The P-V (or△) curve of the specimen obtained from the three-point bending test is shown in Fig.6. It can be seen from Fig.6 (a) that the curve of the sample with the solidification rate of 6 μm/s is wavy at the beginning, which may be caused by the tiny cracks around the cracks when cutting the prefabricated cracks, so that the force is not continuously increased at the beginning of loading. Then, like the other three P-V curves of solidification rate, the uniform rise along a certain slope is basically linear, corresponding to the crack passivation and plastic deformation stage of the sample. Then the curve is accelerated up. The equivalent cross-sectional area is reduced and the flexibility is increased significantly due to the initiation of crack,

Table 2 High temperature fracture toughness of Fe-Al-Ta eutectic under different solidification rate

Solidification rate/(μm/s)	Crack length *a*/mm	P_{max}/P_q	K_q/(MPam$^{1/2}$)	$2.5(K_q/R_{p0.2})^2$/mm	K_{IC}/(MPa·m$^{1/2}$)
6	3.72	1.64	19.3	14.02	Invalid
30	3.69	1.82	17.7	6.46	Invalid
80	3.65	1.46	25.9	12.78	Invalid
200	3.68	1.55	23.7	9.69	Invalid

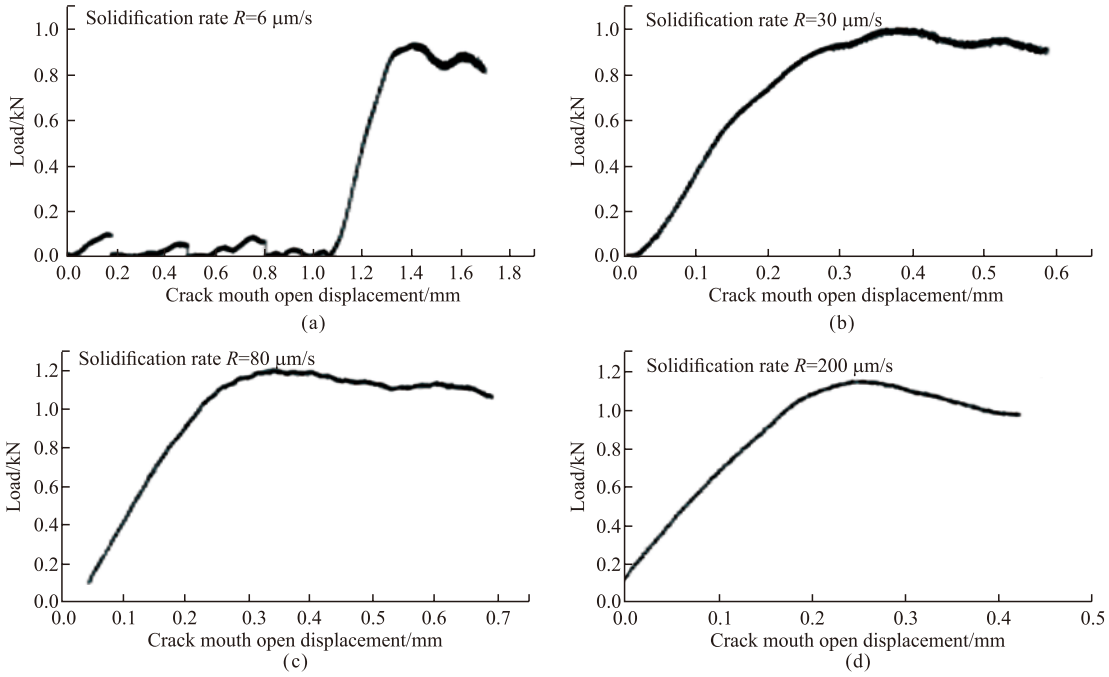

Fig.6 Three-point bending *P-V* curve of Fe-Al-Ta eutectic composites at different solidification rates: (a)6 μm/s; (b)30 μm/s; (c)80 μm/s; (d)200 μm/s

which corresponds to the steady-state growth stage of crack. From Fig.6(a) (b) (c), it can be seen that the wave shape declines after loading to the maximum force. This indicates that the crack growth is blocked and the fracture resistance is large at this time. When the sample force of 200 μm/s is loaded to the maximum value, it drops gently, indicating that the expansion resistance is small.

Fig.7 shows the fracture morphology of Fe-Al-Ta eutectic with the solidification rate of 6 μm/s after the high temperature three-point bending test. Microstructure of Fe-Al-Ta eutectic with the solidification rate of 6 μm/s is regular lamellar, and growth interface is planar interface. The fracture morphology greatly fluctuates at the low-power microscope, indicating that the fracture process is relatively tortuous and the fracture resistance is large. The section is a herringbone, which is composed of the radiation area and the fiber area. Since the solidified structure is lamellar structure at solidification rate of 6 μm/s, Fe_2Ta(Al) phase is a brittle phase. This makes it easy to cause stress concentration. The stress distribution near the crack tip is inhomogeneous during three-point bending test, and the tearing dimple is caused by the non-uniform stress at the crack tip. This indicates that the crack is subjected to some resistance during the propagation. Honeycombed dimples and a small number of pits are visible in Fig.7(d) due to the extraction of Fe_2Ta (Al) fibers. The presence of these dimples indicates that Fe-Al-Ta eutectic has

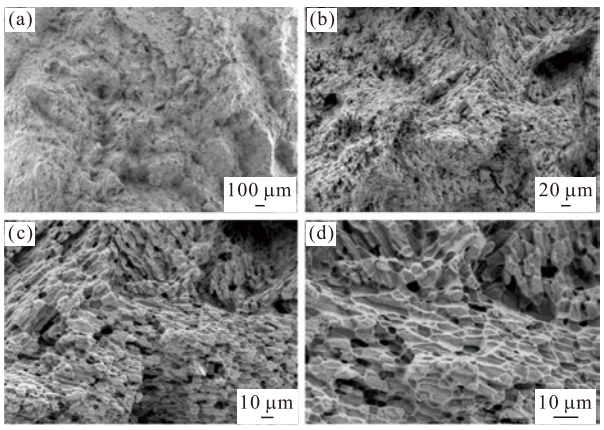

Fig.7 Morphology of Fe-Al-Ta eutectic fracture surface after directional solidification of 6 μm/s: (a)35×; (b)200×; (c)500×; (d)1 000×

ductile fracture characteristics. Therefore, Fe_2Ta (Al) fiber plays a toughening effect in the fracture process of Fe-Al-Ta eutectic sample.

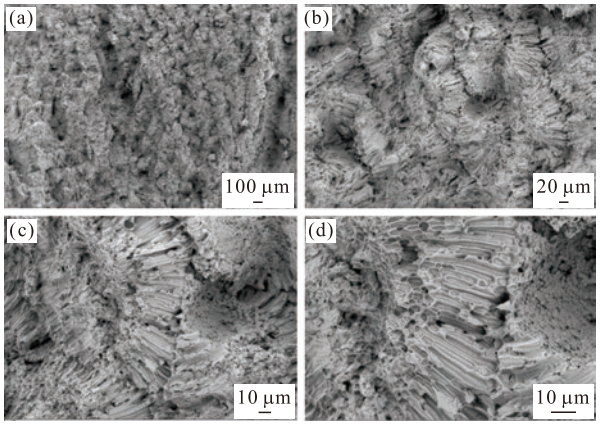

Fig.8 Morphology of Fe-Al-Ta eutectic fracture surface after directional solidification at solidification of 30 μm/s: (a)35×; (b)200×; (c)500×; (d)1 000×

Fig.8 shows the fracture morphology of Fe-Al-Ta eutectic with the solidification rate of 30 μm/s after the high temperature three-point bending test. Microstructure of Fe-Al-Ta eutectic is cellular due to the increase of solidification rate, and the Fe_2Ta (Al)Laves phase with poor orientation accuracy is distributed at the eutectic cell boundary. The cell boundary has less resistance to crack propagation, and the crack is easy to propagate along the eutectic cell boundary. Secondary cracks can be clearly seen at the cell boundary as shown in Fig.8(b). The secondary cracks mainly originate and expand from the cell boundary and absorb less energy during the process of fracture. In the cell boundary, there are thick Fe_2Ta (Al) lamellar structures, while in the cell, there are rod-shaped eutectic with the same orientation, so the deformation modes of the cell boundary and the intracellular stress are different. The microscopic morphology of intracellular fracture is honeycomb. The size of the dimple is small, but the size is basically the same, and the micro pits drawn out by Fe_2Ta (Al) can also be seen.

Fig.9 shows the fracture morphology of Fe-Al-Ta eutectic composites with the solidification rate of 80 μm/s after the high temperature three-point bending test. Structure is refined and the cell size is reduced with solidification rate further increased. Microstructure of the Fe-Al-Ta eutectic is still cellular, and the Fe_2Ta (Al) Laves phase with poor orientation accuracy is distributed at the eutectic cell boundary. The resistance of cell boundary to crack propagation is small and the crack is easy to propagate along the eutectic cell boundary. The section is uneven and the crack extends along the grain boundary. While the inside of the cell is fine rod-like structure, the dimples formed are fine and uniform, and there are almost no secondary cracks observed in the cell.

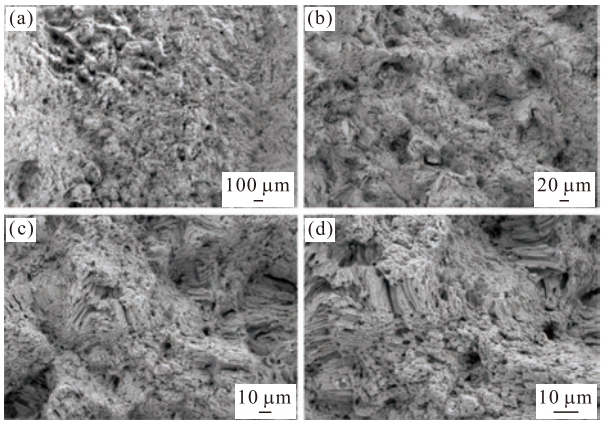

Fig.9 Morphology of Fe-Al-Ta eutectic fracture surface after directional solidification at solidification of 80 μm/s: (a)35×; (b)200×; (c)500×; (d)1 000×

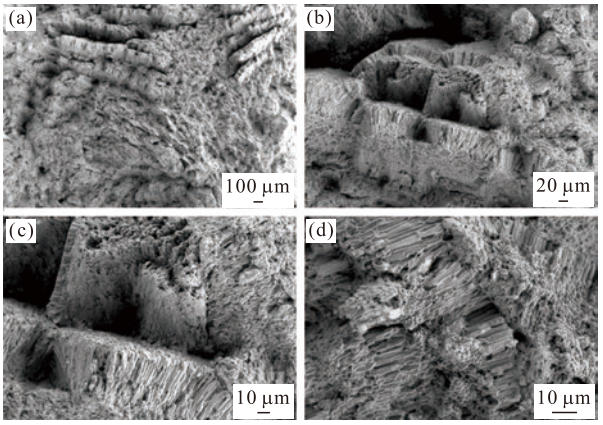

Fig.10 Morphology of Fe-Al-Ta eutectic fracture surface after directional solidification at the solidification rate of 200 μm/s: (a)35×; (b)200×; (c)500×; (d)1 000×

Fig.10 shows the fracture morphology of Fe-Al-Ta eutectic composites with the solidification rate of 200 μm/s after the high temperature three-point bending test. Microstructure of Fe-Al-Ta eutectic significantly refined, and the short lamellar Fe_2Ta (Al) phase at the cell boundary is also refined with the further increase of the solidification rate. There are step shape fractures between the crystal cells as shown in Fig.10(a). As the solidification rate increases, microstructure is refined and the strength in the cell is significantly higher than that in the cell boundary. At the beginning of fracture, radial pattern is found, and then the uneven herringbone ridge pattern can be observed. This may be ascribed to the complex internal stress of the material during the process of indenter pressing, and the formation of micropores at the cell boundary with weak strength,

which eventually leads to the tearing of the material[22].

4 Conclusions

Ta element was added to Fe-Al compound in order to obtain Fe-Al-Ta eutectic by Bridgman directional solidification technique at different solidification rates.

The tensile strength at room temperature is lower than that at the high temperature. The tensile properties of the Fe-Al-Ta eutectic composite are improved with the increase of the solidification rate, which is due to the gradual refinement and specify of the $Fe_2Ta(Al)$ Laves phase with the increase of the solidification rate.

By comparing the tensile and three-point bending fracture toughness of the material at room temperature and 600 ℃, it is found that the fracture is brittle at room temperature and changes into ductile fracture at high-temperature.

References

[1] Sun C, Guo J T, Wang S H, *et al.* Oxidation Behavior of Fe_3Al and FeAl Alloys at High Temperature[J]. *Corrosion Science and Protection Technology*, 1993, 5(2): 110-113

[2] Kai W, Huang R T. The Corrosion Behavior of Fe-Al Alloys in $H_2/H_2S/H_2O$ Atmospheres at 700-900 ℃[J]. *Oxidation of Metals*., 1997, 48(1-2): 59-86

[3] Kumar K S, Bao G. Intermetallic-matrix Composites: An overview[J]. *Composites Science and Technology*, 1994, 52(2): 127-150

[4] Zhou R F, Han Y F, Li S S. *High Temperature Structural Material*[M]. Beijing: National Defense Industry Press, 2006

[5] Guo J T, Zhou L Z, Yuan C, *et al.* Microstructure and Properties of Several Originally Invented and Unique Superalloys in China[J]. *The Chinese Journal of Nonferrous Metals*, 2011, 21(2): 237-25

[6] Yamaguchi M, Inui H, Ito K. High-temperature Structural Intermetallic[J]. *Acta Materialia*, 2000, 48(1): 307-322

[7] Yu X Q, Sun Y S, Mei J P, *et al.* Electrical Properties of Fe_3Al Intermetallic Compounds[J]. *Acta Metallurgical Sinica*, 1998, 34(11): 1 126-1 130

[8] Chen Y H, Xing Z Q. Review and Prospect of Fe_3Al Intermetallic Compounds[J]. *Journal of Beijing University of Technology*, 1996, 22(3): 131-140

[9] Feng X, Jing Y. Contrast Study on The Oxidation Property of 2.25Cr-1Mo and Fe-Al Alloys Under High Temperature[J]. *Journal of Agricultural Mechanization Research*, 2004, (3): 146-147

[10] Liu J, Liu J, Zhou D S. Oxidation Resistance of Fe-Al Intermetallic Containing 21.4 wt%Al at 1250 ℃[J]. *Transactions of Materials and Heat Treatment*, 2009, 30(5): 26-29

[11] Fan R H, Yi Y S, Bi J Q, *et al.* Electron Structures and Intrinsic Brittleness of Fe-25Al Aluminides[J]. *Journal of Synthetic Crystals*, 2002, 31(5): 468-471

[12] Risanti D D, Sauthoff G. Strengthening of Iron Aluminide Alloys by Atomic Ordering and Laves Phase Precipitation for High-temperature Applications[J]. *Intermetallics*, 2005: 1 313-1 321

[13] Pike L M, Liu C T. The Effect of Vacancies on the Environ Mental Yield Strength Dependence of Boron-free and Boron Doped Fe-40Al[J]. *Intermetallics*, 2000(8): 1 413-1 416

[14] Xue F, Sun Y S, Bao Y H, *et al.* Melt Processed Fe_3Al Matrix Composites Reinforced with Ceramic Particles[J]. *Chinese Journal of Materials Research*, 2000, 14(4): 344-348

[15] Zhong Q D, Lei X W, Ji D, *et al.* Advances in the Study of Fe-Al Intermetallic Compounds[J]. *Powder Metallurgy Technology*, 2014, 32(6): 457-463

[16] Reviere R, Sauthoff G, Johnson D R, *et al.* Microstructure of Directionally Solidified Eutectic Based Fe (Al, Ta)/Fe_2Ta (Al) Alloys as a Function of Processing Conditions[J]. *Intermetallics*, 1997, 5: 161-172

[17] Wang P. *The Optimal Orientation and Mechanical Properties of Directionally Solidified Fe-Al-Ta Ternary Alloy*[D]. Xi`an: Xi`an University of Architecture and Technology, 2018

[18] Yang M. *Microstructure Characteristics of Directionally Solidified Fe-Al-Ta Eutectic Alloy*[D]. Xi`an: Xi`an University of Architecture and Technology, 2016

[19] Cui C J, Wang S Y, Yang M, *et al.* Microstructure and Solid/liquid Interface Evolutions of Directionally Solidified Fe-Al-Ta Eutectic Alloy[J]. *Journal of Wuhan University of Technology-Materials Science*, 2019, 34(3): 656-661

[20] Risanti D D, Sauthoff G. Microstructures and Mechanical Properties of Fe-Al-Ta Alloys with Strengthening Laves Phase[J]. *Intermetallics*, 2011, 19: 1 727-1 736

[21] Zhang Z M. *Research on Fracture Toughness of Metal Materials*[D]. Shanghai: Shanghai Jiao Tong University, 2011

[22] Wu G C, Chen G L, Qian W J. *Metal Material Science*[M]. Beijing: Metallurgical Industry press, 2009